Modern Journal of Statistics
1(1), 25–48
DOI: https://doi.org/10.64389/mjs.2025.01109
https://sphinxsp.org/journal/index.php/mjs

Research article

Fitting Real Data Sets by a New Version of Gompertz Distribution

Laxmi Prasad Sapkota[1], Vijay Kumar[2], Getachew Tekle[3*], Hleil Alrweili[4], Manahil SidAhmed Mustafa[5], M. Yusuf[6]

[1]Department of Statistics, Tribhuvan University, Tribhuvan Multiple Campus, Palpa 44600, Nepal; laxmisapkota75@gmail.com

[2]Department of Mathematics and Statistics, DDU Gorakhpur University, Uttar Pradesh 273009, India; vkgkp@rediffmail.com

[3]Department of Statistics, College of natural and Computational Science, Wachemo University, Hosaena 667, Ethiopia; getachewtekle@wcu.edu.et

[4]Department of Mathematics, Faculty of Art and Science, Northern Border University, Arar 1321, Saudi Arabia; Hleil.Alrweili@nbu.edu.sa

[5]Department of Statistics, Faculty of Science, University of Tabuk, Tabuk 71491, Saudi Arabia; msida@ut.edu.sa

[6]Department of Mathematics, Faculty of Science, Helwan University, Cairo 11795, Egypt; mohammed.yousof@yahoo.com

***Correspondence:** getachewtekle@wcu.edu.et

ARTICLE INFO

Keywords: Entropy; Simulation; Gompertz distribution; Moment; Posterior distribution.

Mathematics Subject Classification: 62F10, 62F40, 62E10, 62E15

Important Dates:
Received: 2 June 2025
Revised: 25 June 2025
Accepted: 7 July 2025
Online: 11 July 2025

ABSTRACT

The Poisson Inverted Shifted Gompertz distribution is a new type of distribution that comes from the Poisson-generating family of distributions and is based on the "inverted shifted Gompertz distribution." This distribution has significant statistical characteristics, with clear formulations obtained mathematically. We use three distinct approaches to estimate the parameters of the distribution: maximum likelihood estimation (MLE), least-squares estimation (LSE), and Cramer-Von-Mises estimation (CVME). We undertake a simulation experiment to thoroughly assess the efficacy of maximum likelihood estimation (MLE). Empirical data from engineering and medical fields demonstrate the relevance of our suggested model. We meticulously evaluate the goodness-of-fit of the Poisson Inverted Shifted Gompertz distribution using several statistical tests and graphical techniques. Our suggested distribution demonstrates enhanced fitting capabilities and more flexibility compared to many widely used lifespan distributions. Furthermore, we investigate the Bayesian viewpoint of the proposed model by using Hamiltonian Monte Carlo (HMC) simulation methods. This detailed study gives you a full picture of how the Poisson Inverted Shifted Gompertz distribution can be used in many different areas.

1. Introduction

In the field of statistics, it has become evident that various lifetime distributions have been developed to address the specific needs of different domains such as engineering, medicine, life sciences, risk analysis, and life testing. Classical distributions often fall short when it comes to accommodating real datasets that exhibit significant skewness and kurtosis. Therefore, there is a growing demand for modified distributions capable of better fitting such complex data. A common approach observed in the literature involves the creation of novel distributions by introducing additional parameters, leveraging existing families of distributions, or applying transformations to existing parent distributions. In the present study, we propose a versatile model based on the truncated Poisson family of distributions.

Our research builds upon the work of Kus (2007) [1], who introduced the concept of the truncated Poisson distribution truncated at the origin and define a novel distribution named the Exponential-Poisson (EP) distribution, which exhibits a decreasing hazard rate. The cumulative distribution function (CDF) of the EP distribution is represented as follows:

$$G(t;\beta,\lambda)=\frac{1}{\left(1-e^{-\lambda}\right)}\left[1-\exp\left\{-\lambda\left(1-e^{-\beta t}\right)\right\}\right] \quad ;t>0,(\beta,\lambda)>0\cdot$$

Furthermore, drawing inspiration from the Poisson distribution, (Bereta et al., 2011) [2] presented the Poisson-Weibull distribution. This distribution offers the flexibility of both decreasing and increasing failure rate functions. Additionally, Barreto-Souza and Cribari-Neto (2009) [3] contribute to this growing body of work by introducing the Generalized EP distribution. By inserting a shape parameter to the distribution initially defined by Kus (2007) [1], this distribution exhibits a hazard function with options for increasing, decreasing, or upside-down bathtub-shaped hazard rates.

Extending the same methodology employed in EP, (Cancho, 2011) [4], has presented a novel model capable of accommodating an increasing failure rate function. This model is constructed based on the exponential distribution as the foundational base distribution and is referred to as the Poisson exponential (PE) distribution. Its CDF is represented by

$$G(t;\lambda,\theta)=\frac{e^{-\lambda}-\exp\left\{-\theta\left(1-e^{-\lambda t}\right)\right\}}{\left(1-e^{-\lambda}\right)} \quad ;t>0,\,\lambda,\theta>0\cdot$$

Using the same approach as used by (Cancho, 2011) [4] a two-parameter Poisson-exponential (Louzada-Neto *et al.*, 2011) [5] have studied under the Bayesian approach with the increasing failure rate. A new Poisson generating family of distribution has been developed by (Alkarni & Oraby, 2012) [6] using the truncated Poisson distribution having a decreasing failure rate and its CDF and PDF are,

$$F(x;\lambda,\xi) \;=\; 1\text{-}\frac{1-e^{\lambda[1-G(x;\xi)]}}{(1-e^{-\lambda})};\lambda>0\cdot \tag{1.1}$$

$$f(x;\lambda,\xi)=\frac{\lambda\, g(x;\xi)\; e^{\lambda[1-G(x;\xi)]}}{(1-e^{-\lambda})};\lambda>0, \tag{1.2}$$

where ξ is the parameter space, $g(x;\xi)$ and $G(x;\xi)$ are the PDF and CDF of any arbitrary base distribution.

The Weibull power series family of distributions was introduced by (Morais & Barreto-Souza, 2011) [7], employing the Poisson distribution as its foundation. Subsequently, (Lu & Shi, 2012) [8] generated the Weibull-Poisson model, capable of exhibiting a variety of failure rate hazard functions, including the distinct upside-down bathtub, decreasing, increasing, or unimodal patterns. Mahmoudi and Sepahdar (2013) [9] introduced a novel four-parameter Exponentiated Weibull-Poisson distribution, presented by mixing exponentiated Weibull and Poisson distributions. This distribution also displays bathtub-shaped, increasing, decreasing, or unimodal characteristics. The Weibull-Poisson model in the context of a reliability sampling plan was presented by (Kaviayarasu & Fawaz, 2017) [10]. For software reliability analysis, (Kyurkchiev et al., 2018) [11] defined the exponentiated exponential-Poisson model. Expanding the scope of Poisson-based distributions, (Chaudhary & Kumar, 2020) [12] introduced a flexible model called the Poisson inverse NHE model using the Poisson-G family. In the same year, (Joshi & Kumar, 2020) [13] defined the Poisson exponential power distribution, which was employed to compare various estimation methods for model parameter estimation. Additionally, (Chaudhary et al., 2021) [14] defined another novel distribution, the Poisson Gompertz distribution, within the Poisson family. These developments collectively highlight the motivation and interest in leveraging the Poisson generating family to create innovative and versatile models for various statistical applications. Recently, using the Poissin-G family (Wasinrat, & Choopradit, 2023) [15] defined the new model called Poisson inverse Pareto distribution.

Further we have conducted Bayesian analysis of the proposed model under the HMC technique and presented the results of posterior sampling, its convergence and estimated values of the model parameters. Using the similar approach of Bayesian analysis (Sapkota, 2022) [16] introduced the Weibull Inverse Rayleigh Distribution and analyzed it using HMC technique.

In this paper, we delve into the inverted shifted Gompertz distribution, which is originally defined by (Chaudhary *et al.*, 2020) [17] as an inversion of the well-established shifted Gompertz distribution presented by (Bemmaor, 1994) [18]. The CDF and PDF of the inverted shifted Gompertz distribution, characterized by positive parameters, are given by equations (1.3) and (1.4), respectively.

$$G(x;\alpha,\beta)=1-\left(1-e^{-\beta/x}\right)\exp(-\alpha e^{-\beta/x});\;\; x>0\,. \tag{1.3}$$

$$g(x;\alpha,\beta)=\beta x^{-2}\left\{1+\alpha\left(1-e^{-\beta/x}\right)\right\}\exp\left(-\frac{\beta}{x}-\alpha e^{-\beta/x}\right);\;\; x>0\,. \tag{1.4}$$

Our primary objective in this article is to enhance the versatility of this distribution by introducing a single additional parameter; thereby creating the Poisson inverted shifted Gompertz distribution. The subsequent sections of this paper are organized as follows:

- Section 2 introduces the new Poisson inverted shifted Gompertz distribution model along with its statistical and mathematical properties.

- In Section 3, we present parameter estimation methods, namely the LSE, MLE, and CVME methods.
- Section 4 conducts a simulation study to analyze the behavior of MLEs.
- Section 5 showcases the practical application of the proposed model.
- In Section 6, we present a Bayesian analysis of the suggested model.
- Finally, Section 7 encapsulates the concluding remarks of our study.

2. New distribution

We've introduced a novel model and named the Poisson Inverted Shifted Gompertz (PISG) distribution. This distribution is generated within the Poisson-G family of distributions, as defined in Equation (1.1) and Equation (1.2). To obtain the CDF and PDF for the PISG distribution, we employ Equation (1.3) and Equation (1.4) as a foundational distribution and incorporate them into Equation (1.1) and Equation (1.2). Suppose X is a random variable following the PISG distribution. In that case, we can express the CDF as follows:

$$F(x) = 1 - \frac{1}{(1-e^{-\lambda})}\left[1-\exp\left\{-\lambda\left(1-e^{-\beta/x}\right)\exp(-\alpha e^{-\beta/x})\right\}\right] ;\alpha,\beta,\lambda>0, x>0. \tag{2.1}$$

$$f(x) = \frac{\lambda\beta}{x^2(1-e^{-\lambda})}\left\{1+\alpha\left(1-e^{-\beta/x}\right)\right\}\exp\left(-\frac{\beta}{x}-\alpha e^{-\beta/x}\right)\exp\left\{-\lambda\left(1-e^{-\beta/x}\right)\exp(-\alpha e^{-\beta/x})\right\} ;\alpha,\beta,\lambda>0, x>0. \tag{2.2}$$

The Reliability function of PISG distribution is

$$R(x;\alpha,\beta,\lambda) = \frac{1}{(1-e^{-\lambda})}\left[1-\exp\left\{-\lambda\left(1-e^{-\beta/x}\right)\exp(-\alpha e^{-\beta/x})\right\}\right]; x>0 \cdot \tag{2.3}$$

The Hazard rate function (HRF) of the proposed model is,

$$h(x) = \beta\lambda x^{-2}\left\{1+\alpha\left(1-e^{-\beta/x}\right)\right\}\exp\left(-\frac{\beta}{x}-\alpha e^{-\beta/x}\right)\frac{D(x)}{1-D(x)}; x>0, \tag{2.4}$$

where $D(x) = \exp\left\{-\lambda\left(1-e^{-\beta/x}\right)\exp(-\alpha e^{-\beta/x})\right\}$.

Figure 1 illustrates the diverse patterns observed in the hazard function and PDF of the PISG distribution. The hazard function graph showcases a range of shapes, including monotonically non-decreasing, and an inverted bathtub, each corresponding to different values of the parameters. Meanwhile, the PDF graph provides evidence that the proposed model exhibits a right-skewed distribution.

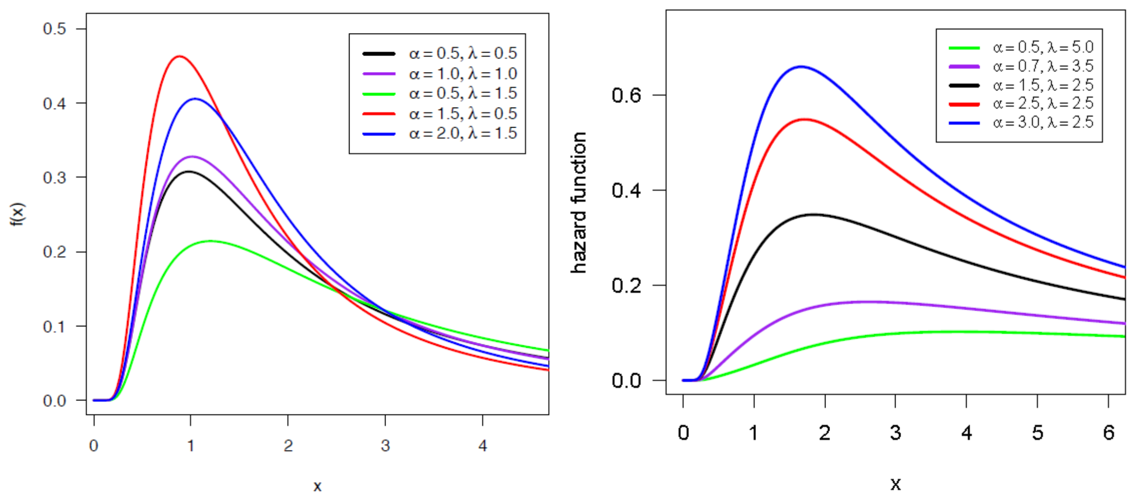

Figure 1. Graph of HRF (right panel) and PDF (left panel) for different values of α and λ keeping fixed β.

The expression for Quantile function (QF) is

$$\alpha\exp(-\beta/x) - \ln\{1-\exp(-\beta/x)\} + \ln(1-z) = 0, \tag{2.5}$$

$$where,\ z = 1+\frac{1}{\lambda}\log\left[1-(1-e^{-\lambda})(1-p)\right];\ 0<p<1.$$

To generate the random numbers from the PISG distribution, we can use

$$\begin{aligned}&\alpha\exp\left(-\beta/x\right)+\ln(1-z)\text{-}\ln\left\{1-\exp\left(-\beta/x\right)\right\}=0,\\&where,\ z=1+\frac{1}{\lambda}\log\left\{1-(1-e^{-\lambda})(1-u)\right\};\ 0<u<1\end{aligned} \quad . \tag{2.6}$$

Based on the QF function defined in (2.5), the coefficient of skewness of the PISG distribution can be calculated as

$$S_k\left(B\right)=\frac{Q\left(3/4\right)+Q\left(1/4\right)-2Q\left(1/2\right)}{Q\left(3/4\right)-Q\left(1/4\right)} \text{ and}$$

The coefficient of kurtosis is

$$K_u\left(M\right)=\frac{Q\left(0.875\right)-Q\left(0.625\right)+Q\left(0.375\right)-Q\left(0.125\right)}{Q\left(0.75\right)-Q\left(0.25\right)}.$$

2.1. Some useful expansions and properties of PISG distribution

Here we have expanded the CDF and PDF of PISG distribution by using the following series expansions

$$\left(1-a\right)^d = \sum_{j=0}^{\infty}(-1)^j\binom{d}{j}\mathrm{a}^j .$$

$$e^{-z} = \sum_{a=0}^{\infty}\frac{\left(-1\right)^a z^a}{a!} .$$

Expansion of the CDF of PISG distribution defined in Equation (2.1) is

$$F\left(x;\alpha,\beta,\lambda\right)= C+\sum_{i=0}^{\infty}\sum_{j=0}^{\infty}\sum_{k=0}^{n}B_{ijk}e^{-\beta(j+k)/x};x>0. \tag{2.7}$$

where $C=1\text{-}\frac{1}{(1-e^{-\lambda})}$ *and* $B_{ijk}=\frac{(-1)^{i+j+k}\lambda^i\alpha^k\binom{i}{j}}{i!k!(1-e^{-\lambda})}$.

Using the Equation (2.7), the linear form of the PDF can be obtained as

$$\begin{aligned}f(x;\alpha,\beta,\lambda) &= \sum_{i=0}^{\infty}\sum_{j=0}^{\infty}\sum_{k=0}^{n}B_{ijk}e^{-\beta(j+k)/x}\frac{\beta(k+j)}{x^2}\\&=\sum_{i=0}^{\infty}\sum_{j=0}^{\infty}\sum_{k=0}^{n}B_{ijk}\,f^*\left[x;\beta\left(k+j\right),\,1\right],\end{aligned} \tag{2.8}$$

where $f^*\left[x;\beta\left(k+j\right),\,1\right]$ is the PDF of inverse Weibull distribution having scale and shape parameters $\beta\left(k+j\right)$ and 1 respectively. Also using Equation (2.8) we can express the PDF as

$$f\left(x\right)= \sum_{i=0}^{\infty}\sum_{j=0}^{\infty}\sum_{k=0}^{n}B'_{ijk}\ x^{-2}e^{-\beta(k+j)/x} \tag{2.9}$$

where $B'_{ijk}=B_{ijk}\times\beta(k+j)$.

Moment is an important tool in the probability theory and it is used to compute various orders of the moments. Using the PDF defined in Equation (2.9), r$^{\text{th}}$ raw moment of PISG distribution can be expressed as

$$\begin{aligned}\mu'_r &= \int_0^{\infty}x^r\ \sum_{i=0}^{\infty}\ \sum_{j=0}^{\infty}\ \sum_{k=0}^{n}\ B'_{ijk}\ x^{-2}e^{-\beta(j+k)/x}dx\\&=\sum_{i=0}^{\infty}\ \sum_{j=0}^{\infty}\ \sum_{k=0}^{n}\ B'_{ijk}\ \frac{\Gamma\left(1-r\right)}{\left[\beta(j+k)\right]^{1-r}}\end{aligned} \tag{2.10}$$

where $\int_0^{\infty}x^n e^{-ax}dx=\frac{\Gamma\left(n+1\right)}{a^{n+1}}$ is a standard gamma integral.

The Moment Generating Function (mgf) of $X\sim PISG\left(\alpha,\beta,\lambda\right)$ using Equation (2.10) can be expressed as

$$M_X\left(t\right)=\sum_{i=0}^{\infty}\sum_{j=0}^{\infty}\sum_{k=0}^{n}\sum_{l=0}^{\infty}B'_{ijk}\ \frac{t^l}{l!}\frac{\Gamma\left(1-r\right)}{\left[\beta(j+k)\right]^{1-r}}.$$

The conditional moments of $X\sim PISG\left(\alpha,\beta,\lambda\right)$ with PDF defined in Equation (2.9) can be presented as

$$E\left(X^n / X > x\right) = \frac{1}{S(x)} \sum_{i=0}^{\infty} \sum_{j=0}^{\infty} \sum_{k=0}^{n} B'_{ijk} \frac{\Gamma\{1-n, \beta(j+k)x\}}{[\beta(j+k)]^{1-n}}. \tag{2.11}$$

S(x) is the survival function and $\int_t^{\infty} x^a e^{-bx} dx = \frac{\Gamma(a+1, bt)}{b^{a+1}}$ is the upper incomplete gamma function.

The Average Residual Life (ARL) function of X using PDF referred in Equation (2.9) can be expressed as

$$\mu_x(x) = \frac{\sum_{i=0}^{\infty} \sum_{j=0}^{\infty} \sum_{k=0}^{n} B'_{ijk} \, \Gamma\{2, \beta(j+k)x\}}{S(x)\{\beta(j+k)\}^2} - x.$$

Entropies are also useful statistical tools for determining the randomness and uncertainty of any event or system's random observations. We calculated the q and Renyi entropies in this article, which are as follows:

a) **Renyi entropy**: It can be defined as

$$R_\eta(x) = \frac{1}{1-\eta} \ln\left[\int_0^{\infty} \{f(x)\}^\eta \, dx\right]; \eta > 0, \eta \neq 1. \tag{2.12}$$

By expanding the term $\{f(x)\}^\eta$ where $f(x)$ is the PDF defined in Equation (2.2) and we can write

$$\{f(x)\}^\eta = \sum_{i=0}^{\eta} \sum_{j=0}^{\infty} \sum_{k=0}^{\infty} \sum_{l=0}^{\infty} \sum_{m=0}^{\infty} \sum_{p=0}^{\infty} \sum_{q=0}^{i} \Phi_{ijklmpq} x^{-2\eta-i+q} e^{-\frac{\beta}{x}(p+q+l+m)} \tag{2.13}$$

where $\Phi_{ijklmpq} = \left[\frac{\alpha\beta}{1-e^{-\lambda}}\right]^\eta \alpha^{i+q} \eta^q (\beta\eta)^{i-q} \binom{\eta}{i}\binom{i}{p}\binom{i}{q}(-1)^{j+q} D_{klm}$ and $D_{klm} = \frac{(-1)^{k+l+m} \lambda^k \alpha^m \binom{k}{l}}{k!m!}$.

Using Equation (2.13) in Equation (2.12) we find the Renyi entropy as

$$R_\eta(x) = \frac{1}{1-\eta} \ln\left[\sum_{i=0}^{\eta} \sum_{j=0}^{\infty} \sum_{k=0}^{\infty} \sum_{l=0}^{\infty} \sum_{m=0}^{\infty} \sum_{p=0}^{\infty} \sum_{q=0}^{i} \Phi_{ijklmpq} \frac{\Gamma(2\eta - q + i - 1)}{\{\beta(p+q+l+m)\}^{2\eta-q+i-1}}\right].$$

b) q-Entropy: Similarly, the q-entropy for $X \sim PISG(\alpha, \beta, \lambda)$ can be expressed as

$$W_c(x) = \frac{1}{1-c} \ln\left[1 - \int_0^{\infty} \{f(x)\}^c \, dx\right]; c > 0, c \neq 1.$$

Hence q-entropy for the proposed distribution PISG can be expressed by performing similar steps as Renyi entropy,

$$W_c(x) = \frac{1}{1-c} \ln\left[1 - \sum_{i=0}^{c} \sum_{j=0}^{\infty} \sum_{k=0}^{\infty} \sum_{l=0}^{\infty} \sum_{m=0}^{\infty} \sum_{p=0}^{\infty} \sum_{q=0}^{i} \Phi_{ijklmpq} \frac{\Gamma(2c - q + i - 1)}{\{\beta(p+q+l+m)\}^{2c-q+i-1}}\right]; c > 0, c \neq 1.$$

Let $X_{k:n}$ represents the kth OS and $f_{k:n}$ indicate PDF of Kth Order Statistics (OS) of PISG distribution for ordered variables $X_1, \dots, X_n$ from $F(x)$, can be expressed as

$$f_{k:n}(x) = \frac{n!}{(k-1)!(n-k)!} f(x)\left[F(x)\right]^{k-1}\left[1 - F(x)\right]^{n-k}$$
$$= \frac{n!}{(k-1)!(n-k)!} f(x) \sum_{j=1}^{n-k} \binom{n-k}{j} \left[F(x)\right]^{j+k-1}.$$

Using the Equations (2.7) and (2.9) we get

$$= \sum_{i=0}^{\infty} \sum_{j=0}^{\infty} \sum_{k=0}^{n} B'_{ijk} \, x^{-2} e^{-\beta(j+k)/x} \sum_{l=1}^{n-k} \binom{n-k}{l} \left[\mathrm{C} + \sum_{i=0}^{\infty} \sum_{j=0}^{\infty} \sum_{k=0}^{n} B_{ijk} e^{-\beta(j+k)/x}\right]^{l+k-1}, \tag{2.14}$$

where $B^*_{ijk} = B'_{ijk} \times \frac{n!}{(k-1)!(n-k)!}$.

Now the jth moment of kth OS can be computed as

$$E\left(X_{(k)}^{j}\right)=\int_{0}^{\infty} x_{(k)}^{j} f_{k:n}\left(x_{(k)}\right) dx_{(k)}.$$

Using the Equation (2.14) we get the kth order statistics.

3. Parameter Estimation and Inference

The proposed model's parameters are determined through the utilization of three distinct estimation techniques:

a) MLE method
b) LSE method
c) CVM estimation method

3.1. MLE method

Let a random sample of size n be $\underset{\sim}{x} = (x_1,\ldots,x_n)$ from $PISG(\alpha,\ \beta,\ \lambda)$ then the log-likelihood density can be presented as

$$\ell = n\left\{\log(\beta\lambda)-\log(1-e^{-\lambda})\right\}-2\sum_{i=1}^{n}\log x_i+\sum_{i=1}^{n}\log\left\{1+\alpha\left(1-e^{-\beta/x_i}\right)\right\}-\beta\sum_{i=1}^{n}\frac{1}{x_i} \qquad (3.1)$$
$$-\alpha\sum_{i=1}^{n}e^{-\beta/x_i}-\lambda\sum_{i=1}^{n}\left(1-e^{-\beta/x_i}\right)\exp(-\alpha e^{-\beta/x_i}).$$

By differentiating Equation (3.1) w. r. t. model parameters we get

$$\frac{\partial l}{\partial\alpha}=\sum_{i=1}^{n}\frac{1-e^{-\beta/x_i}}{1+\alpha\left(1-e^{-\beta/x_i}\right)}-\sum_{i=1}^{n}e^{-\beta/x_i}+\lambda\sum_{i=1}^{n}e^{-\beta/x_i}\left(1-e^{-\beta/x_i}\right)\exp(-\alpha e^{-\beta/x_i}),$$

$$\frac{\partial l}{\partial\beta}=\frac{n}{\beta}+\alpha\sum_{i=1}^{n}\frac{x_i^{-1}e^{-\beta/x_i}}{1+\alpha\left(1-e^{-\beta/x_i}\right)}-\sum_{i=1}^{n}\frac{1}{x_i}+\alpha\sum_{i=1}^{n}x_i^{-1}e^{-\beta/x_i}+\alpha\lambda\sum_{i=1}^{n}e^{-2\beta/x_i}x_i^{-1}\exp(-\alpha e^{-\beta/x_i}),$$

$$\frac{\partial l}{\partial\lambda}=\frac{n}{\lambda}+\frac{ne^{-\lambda}}{1-e^{-\lambda}}-\sum_{i=1}^{n}\left(1-e^{-\beta/x_i}\right)\exp(-\alpha e^{-\beta/x_i}).$$

To obtain the MLEs for the parameters of the PISG distribution, we typically need to solve a set of non-linear equations. However, solving these equations numerically can be challenging, and it is often more convenient to employ computer software such as R, Python, Mathematica, or Matlab.

If we denote the vector of parameters as $\underset{\sim}{\pi}=(\alpha,\beta,\lambda)$ and their corresponding MLEs as $\hat{\underset{\sim}{\pi}}=(\hat{\alpha},\hat{\beta},\hat{\lambda})$, then $(\hat{\underset{\sim}{\pi}}-\underset{\sim}{\pi})\rightarrow N_3\left[0,\left(H\left(\underset{\sim}{\pi}\right)\right)^{-1}\right]$ follows a normal distribution. This distribution is characterized by its mean, which equals 0, and its variance-covariance matrix, which is derived from the Fisher's information matrix (FIM) denoted as $H\left(\underset{\sim}{\pi}\right)$ and it can be computed as

$$H=\begin{bmatrix} H_{11} & H_{12} & H_{13}\\ H_{21} & H_{22} & H_{23}\\ H_{31} & H_{32} & H_{33}\end{bmatrix}.$$

where $H_{11}=\frac{\partial^2 l}{\partial\alpha^2}$, $\mathrm{H}_{12}=\frac{\partial^2 l}{\partial\alpha\partial\beta}$, $\mathrm{H}_{13}=\frac{\partial^2 l}{\partial\alpha\partial\lambda}$,
$H_{21}=\frac{\partial^2 l}{\partial\beta\partial\alpha}$, $\mathrm{H}_{22}=\frac{\partial^2 l}{\partial\beta^2}$, $\mathrm{H}_{23}=\frac{\partial^2 l}{\partial\beta\partial\lambda}$,
$H_{31}=\frac{\partial^2 l}{\partial\lambda\partial\alpha}$, $\mathrm{H}_{32}=\frac{\partial^2 l}{\partial\beta\partial\lambda}$, $\mathrm{H}_{33}=\frac{\partial^2 l}{\partial\lambda^2}$.

The asymptotic variance $\left(H\left(\underset{\sim}{\pi}\right)\right)^{-1}$ of the MLE is generally not directly useful since it is rarely known in practice. To approximate it, we substitute the estimated parameter values into the FIM. By applying an appropriate optimization method, such as the Newton-Raphson algorithm, to maximize the likelihood function, we obtain the observed FIM. The variance-covariance matrix can then be derived from this as

$$\left(H(\underline{\pi})\right)^{-1}=\begin{pmatrix} V(\hat{\alpha}) & \operatorname{cov}(\hat{\alpha},\hat{\beta}) & \operatorname{cov}(\hat{\alpha},\hat{\lambda}) \\ \operatorname{cov}(\hat{\beta},\hat{\alpha}) & V(\hat{\beta}) & \operatorname{cov}(\hat{\beta},\hat{\lambda}) \\ \operatorname{cov}(\hat{\lambda},\hat{\alpha}) & \operatorname{cov}(\hat{\lambda},\hat{\beta}) & V(\hat{\lambda}) \end{pmatrix}. \tag{3.2}$$

Utilizing equation (3.2), we can construct 100(1-τ)% confidence intervals for the following parameters of the PSIG model:

$$\hat{\alpha}\pm Z_{\tau/2}SE(\hat{\alpha})\ ,\ \hat{\beta}\pm Z_{\tau/2}SE(\hat{\beta})\text{ and, }\hat{\lambda}\pm Z_{\tau/2}SE(\hat{\lambda}).$$

3.2. Method of Least-Square Estimation (LSE)

The LSE method can be employed as another technique for estimating the unknown parameters α, β, and λ within the context of the PISG distribution. To calculate these parameters, we utilize a minimization approach applied to the function

$$J(X;\alpha,\beta,\lambda)=\sum_{i=1}^{n}\left[F(X_{(i)})-\frac{i}{n+1}\right]^2. \tag{3.3}$$

This minimization is carried out with respect to the aforementioned unknown constants α, β, and λ.

Let's denote $F(X_{(i)})$ as the CDF of the ordered rv $X_{(1)}<\ldots<X_{(n)}$, where $\{X_1,\ldots,X_n\}$ represents a sample of size n drawn from F(.). The LSEs can be computed by minimizing the function

$$J(X)=\sum_{i=1}^{n}\left[1-\frac{1}{(1-e^{-\lambda})}\left[1-D(x_{(i)})\right]-\frac{i}{n+1}\right]^2 \tag{3.4}$$

with respect to the parameters of the PISG model. Differentiating Equation (3.4) with respect to α, β and λ we get,

$$\frac{\partial J}{\partial\alpha}=\frac{2\lambda}{(1-e^{-\lambda})}\sum_{i=1}^{n}\left[1-\frac{1}{(1-e^{-\lambda})}\left[1-D(x_i)\right]-\frac{i}{n+1}\right]\times D(x_i)\left(1-e^{-\beta/x_i}\right)e^{-\beta/x_i}\exp(-\alpha e^{-\beta/x_i})$$

$$\frac{\partial J}{\partial\beta}=\frac{2\alpha\lambda}{(1-e^{-\lambda})}\sum_{i=1}^{n}x_i^{-1}e^{-2\beta/x_i}\exp(-\alpha e^{-\beta/x_i})\left[1-\frac{1}{(1-e^{-\lambda})}\left[1-D(x_i)\right]-\frac{i}{n+1}\right]D(x_i)$$

$$\frac{\partial J}{\partial\lambda}=-2\sum_{i=1}^{n}\left[1-\frac{1}{(1-e^{-\lambda})}\left[1-D(x_i)\right]-\frac{i}{n+1}\right]\left[\frac{1}{(1-e^{-\lambda})}D(x_i)\left(1-e^{-\beta/x_i}\right)\exp(-\alpha e^{-\beta/x_i})-\frac{e^{-\lambda}}{(1-e^{-\lambda})^2}\{1-D(x_i)\}\right]$$

where $D(x_i)=\exp\left\{-\lambda\left(1-e^{-\beta/x_i}\right)\exp(-\alpha e^{-\beta/x_i})\right\}$. After solving above three equations we can obtained the LSEs.

3.3. CVM Estimation Method

The CVME of α, β and λ can be calculated by minimizing the following function

$$I(X)=\frac{1}{12n}+\sum_{i=1}^{n}\left[F(x_{i:n}\,|\,\alpha,\beta,\lambda)-\frac{2i-1}{2n}\right]^2$$

$$=\frac{1}{12n}+\sum_{i=1}^{n}\left[1-\frac{1}{(1-e^{-\lambda})}\left[1-D\left(x_{(i)}\right)\right]-\frac{2i-1}{2n}\right]^2. \tag{3.5}$$

Differentiating Equation (3.5) with respect to α, β and λ we get,

$$\frac{\partial I}{\partial\alpha}=\frac{2\lambda}{(1-e^{-\lambda})}\sum_{i=1}^{n}\left[1-\frac{1}{(1-e^{-\lambda})}\left[1-D(x_i)\right]-\frac{2i-1}{2n}\right]D(x_i)\left(1-e^{-\beta/x_i}\right)e^{-\beta/x_i}\exp(-\alpha e^{-\beta/x_i})$$

$$\frac{\partial I}{\partial \beta}=\frac{2\alpha\lambda}{(1-e^{-\lambda})}\sum_{i=1}^{n} x_i^{-1}e^{-2\beta/x_i}\exp(-\alpha e^{-\beta/x_i})D(x_i)$$
$$\left[1\text{-}\frac{1}{(1-e^{-\lambda})}\left[1-D(x_i)\right]-\frac{2i-1}{2n}\right]$$
$$\frac{\partial I}{\partial \lambda}=-2\sum_{i=1}^{n}\left[1\text{-}\frac{1}{(1-e^{-\lambda})}\left[1-D(x_i)\right]-\frac{2i-1}{2n}\right]$$
$$\left[\frac{1}{(1-e^{-\lambda})}D(x_i)\left(1-e^{-\beta/x_i}\right)\exp(-\alpha e^{-\beta/x_i})-\frac{e^{-\lambda}}{(1-e^{-\lambda})^2}\{1-D(x_i)\}\right],$$

where $D(x_i)=\exp\left\{-\lambda\left(1-e^{-\beta/x_i}\right)\exp(-\alpha e^{-\beta/x_i})\right\}$. After solving non-linear equations $\frac{\partial I}{\partial \alpha}=0, \frac{\partial I}{\partial \beta}=0$ *and* $\frac{\partial I}{\partial \lambda}=0$ we will get the CVM estimators.

4. Simulation study

We carried out a simulation experiment to assess the practical performance of MLEs in the context of the PISG distribution. These MLEs were computed using the **maxLik ()** package within the R programming software. In our simulation study, we considered a range of sample sizes (n = 50, 70, 100, 150, 200, 250, 300, 350, 400, 450, 500, 600, 700, 800, and 1000) with initial parameter values set1= $\alpha=100,\ \beta=10$ and $\lambda=2$, set2 = $\alpha=120,\ \beta=5$ and $\lambda=2.5$, set3 = $\alpha=80,\ \beta=5$ and $\lambda=0.25$ and set4 = $\alpha=25,\ \beta=2$ and $\lambda=0.15$. For each of these sample sizes, we repeated the experiment 10000 times to obtain robust results. The outcomes of simulation experiment are presented in Tables 1 to 12.

Figures 2-5 displays the graphical representation of the average bias (referred to as 'bias') and the mean square errors (referred to as 'MSEs') for each parameter of interest. Notably, our observations revealed a clear trend: as the sample size increased, both bias and MSEs decreased, aligning with our expectations (see Figures 2-5).

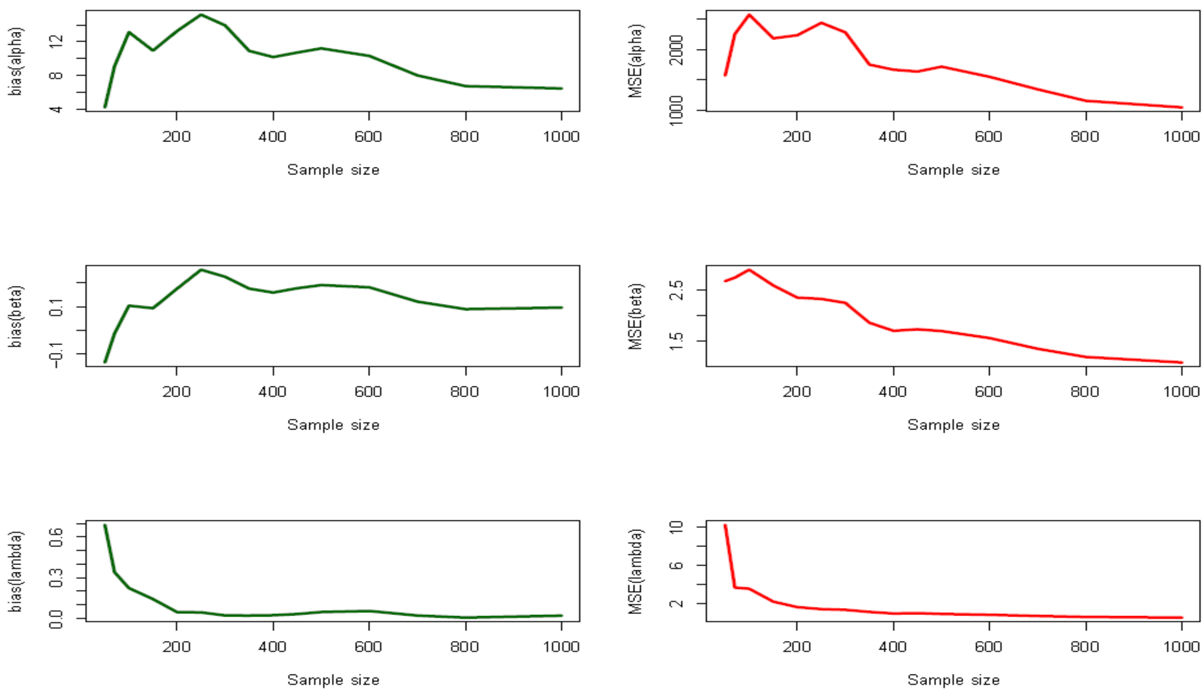

Figure 2: Graph of Biases and MSEs for set1 for various sizes of samples.

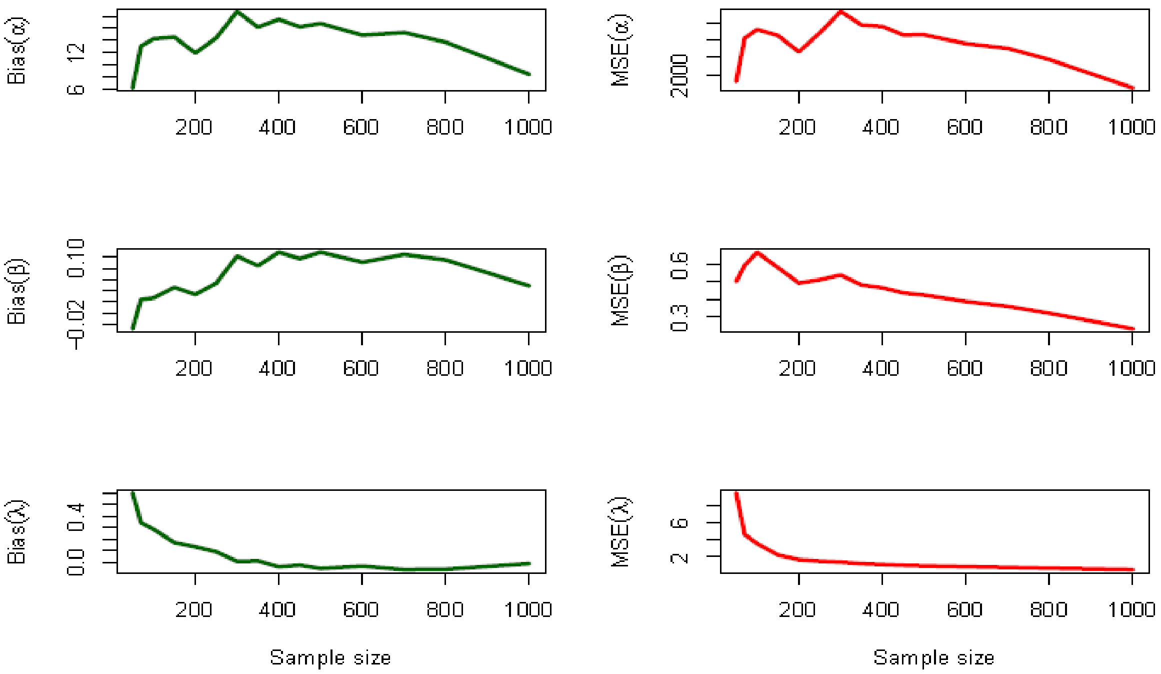

Figure 3: Graph of Biases and MSEs for set2 for various sizes of samples.

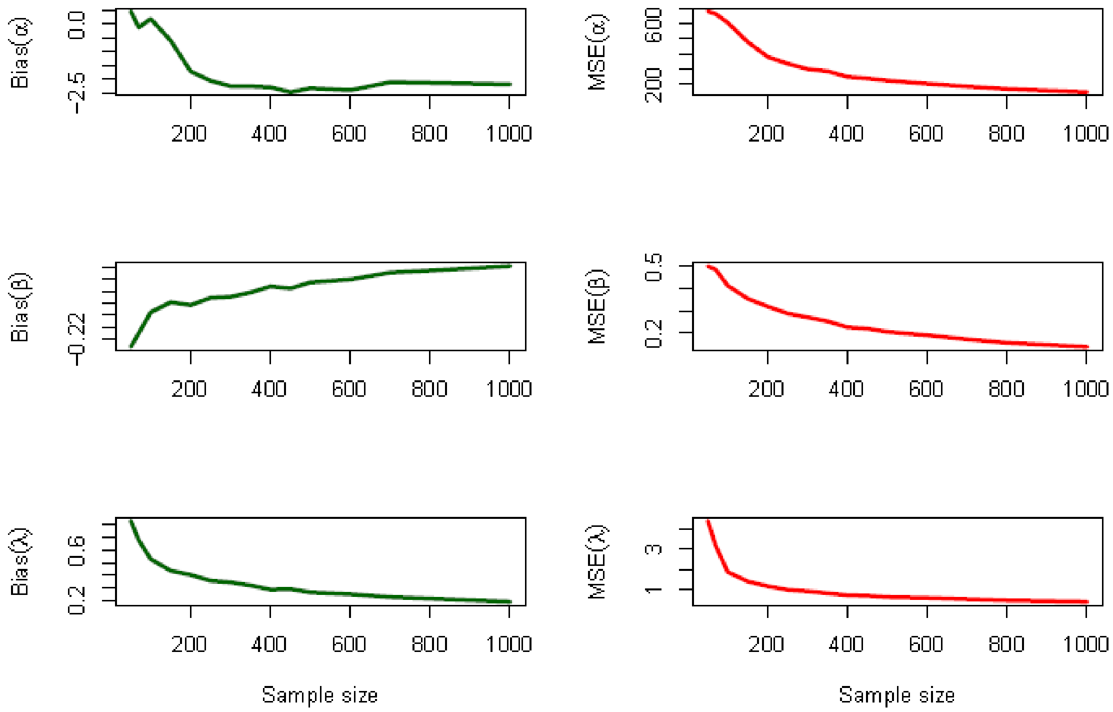

Figure 4: Graph of Biases and MSEs for set3 for various sizes of samples.

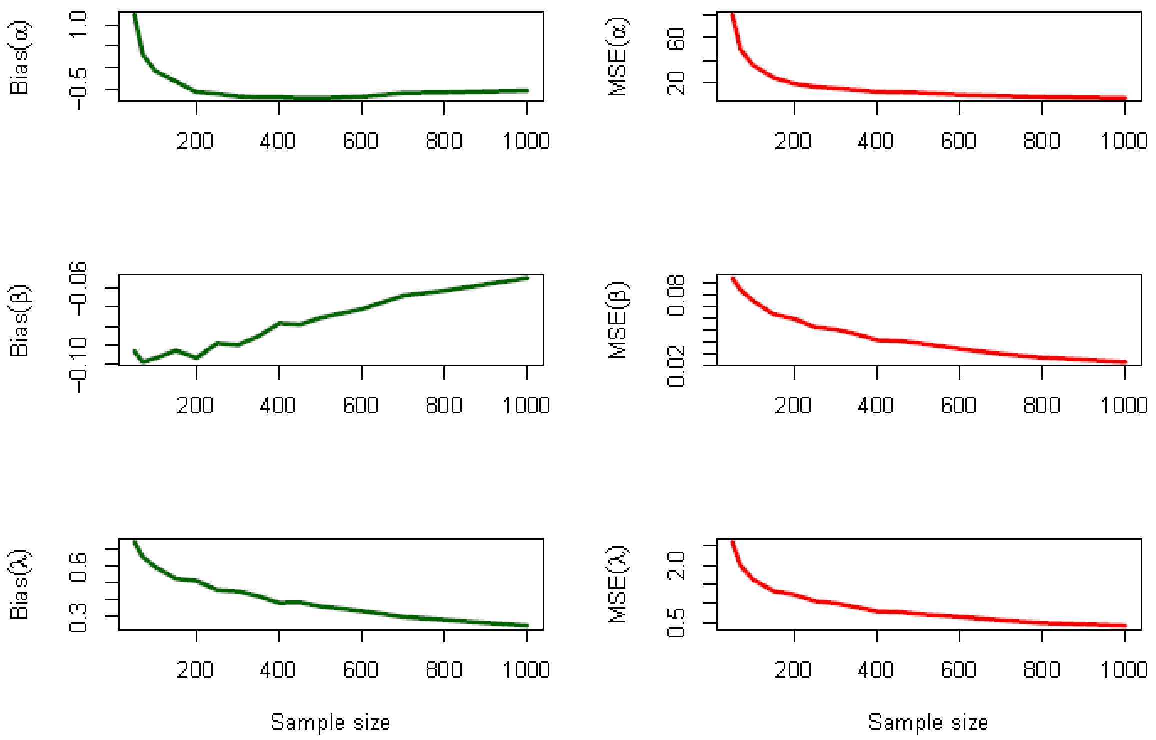

Figure 5: Graph of Biases and MSEs for set4 for various sizes of samples.

Table 1. Simulation Data for Alpha (set1)

Sample size	MLE	Bias	MSE
50	104.1634	4.1634	1572.4358
70	109.0658	9.0658	2247.2701
100	113.1358	13.1358	2564.1945
150	110.9393	10.9393	2178.807
200	113.2688	13.2688	2229.1124
250	115.2261	15.2261	2431.2954
300	113.9418	13.9418	2275.0721
350	110.904	10.904	1750.4356
400	110.1681	10.1681	1668.4942
450	110.7067	10.7067	1638.3774
500	111.2024	11.2024	1718.0588
600	110.3047	10.3047	1551.87043
700	107.9789	7.9789	1348.4131
800	106.704	6.704	1162.2262
1000	106.425	6.425	1054.6238

Table 2. Simulation data for Beta (set1)

Sample size	MLE	Bias	MSE
50	9.8642	-0.1358	2.6692
70	9.9862	-0.01383	2.7360
100	10.1037	0.1037	2.8904
150	10.0929	0.0929	2.5844
200	10.1751	0.1751	2.3474
250	10.2551	0.2551	2.3225
300	10.2254	0.2254	2.2451
350	10.1756	0.1756	1.8572
400	10.1590	0.1590	1.7017
450	10.1771	0.1771	1.7309
500	10.1904	0.1904	1.6966
600	10.1811	0.1811	1.5597
700	10.1206	0.1206	1.3514
800	10.0889	0.0889	1.1921
1000	10.0957	0.0957	1.0843

Table 3. Simulation data for Lambda (set1)

Sample size	MLE	Bias	MSE
50	2.6894	0.6894	10.2365
70	2.3403	0.3403	3.6945
100	2.2331	0.2231	3.5704
150	2.1420	0.1420	2.2252
200	2.0461	0.0461	1.6522
250	1.9560	-0.0440	1.4460
300	1.9705	-0.0215	1.3717
350	1.9789	-0.0210	1.1506
400	1.9768	-0.0232	0.9874
450	1.9680	-0.0319	1.0287
500	1.9533	-0.0467	0.9400
600	1.9456	-0.0544	0.8554
700	1.9791	-0.0208	0.7280
800	1.9943	-0.0057	0.6304
1000	1.9799	-0.0200	0.5604

Table 4. Simulation Data for Alpha (set2)

Sample size	MLE	Bias	MSE
50	126.2087	6.2087	1795.716
70	133.0813	13.0812	3060.706
100	134.2783	14.2783	3317.215
150	134.5725	14.5725	3139.372
200	131.9569	11.9569	2666.325
250	134.4178	14.4178	3219.129
300	138.7704	18.7703	3844.517
350	136.2224	16.2223	3452.874
400	137.4809	17.4809	3408.507
450	136.2686	16.2685	3156.607
500	136.8147	16.8146	3160.86
600	134.8815	14.8814	2905.481
700	135.3107	15.3107	2766.600
800	133.7233	13.7233	2435.183
1000	128.427	8.4270	1606.865

Table 5. Simulation Data for Beta (set2)

Sample size	MLE	Bias	MSE
50	4.9719	-0.0280	0.5016
70	5.0241	0.0241	0.5932
100	5.0269	0.0269	0.6681
150	5.0458	0.0458	0.5802
200	5.0331	0.0331	0.4922
250	5.0533	0.0533	0.5111
300	5.1017	0.1017	0.5378
350	5.0846	0.0846	0.4811
400	5.1084	0.1084	0.4648
450	5.0973	0.0973	0.4352
500	5.1085	0.1085	0.4229
600	5.0910	0.0910	0.3865
700	5.1045	0.1045	0.3587
800	5.0949	0.0949	0.3187
1000	5.0485	0.0485	0.2302

Table 6. Simulation Data for Lambda (set2)

Sample size	MLE	Bias	MSE
50	3.1010	0.6010	9.4990
70	2.8425	0.3425	4.6394
100	2.7844	0.2844	3.5575
150	2.6681	0.1681	2.2110
200	2.6310	0.1310	1.6749
250	2.5872	0.0872	1.5001
300	2.5038	0.0038	1.3908
350	2.5083	0.0083	1.2109
400	2.4575	-0.0424	1.1130
450	2.4711	-0.0288	1.0143

500	2.4419	-0.0580	0.9500
600	2.4625	-0.0374	0.8548
700	2.4319	-0.0680	0.7668
800	2.4353	-0.0646	0.6713
1000	2.4850	-0.0149	0.5037

Table 7. Simulation Data for Alpha (set3)

Sample size	MLE	Bias	MSE
50	80.4448	0.4448	682.5403
70	79.8619	-0.1380	664.7163
100	80.1707	0.1707	607.0691
150	79.3822	-0.6177	478.9579
200	78.2687	-1.7312	379.3183
250	77.9301	-2.0699	334.9133
300	77.7339	-2.2660	299.6260
350	77.7302	-2.2697	284.4084
400	77.6952	-2.3047	247.6726
450	77.5188	-2.4812	236.9610
500	77.6599	-2.3400	223.0173
600	77.5914	-2.4085	201.8562
700	77.8801	-2.1198	183.3179
800	77.8555	-2.1444	167.4643
1000	77.8003	-2.1996	146.0125

Table 8. Simulation Data for Beta (set3)

Sample size	MLE	Bias	MSE
50	4.7667	-0.2332	0.4997
70	4.7896	-0.2103	0.4834
100	4.8246	-0.1753	0.4116
150	4.8413	-0.1586	0.3531
200	4.8365	-0.1634	0.3179
250	4.8486	-0.1513	0.2865
300	4.8503	-0.1497	0.2692
350	4.8575	-0.1424	0.2513
400	4.8676	-0.1323	0.2246
450	4.8642	-0.1357	0.2183
500	4.8743	-0.1256	0.2039
600	4.8792	-0.1207	0.1887
700	4.8907	-0.1092	0.1704
800	4.8940	-0.1059	0.1546
1000	4.9015	-0.0984	0.1363

Table 9. Simulation Data for Lambda (set3)

Sample size	**MLE**	**Bias**	**MSE**
50	1.0834	0.8334	4.3990
70	0.9283	0.6783	3.1555
100	0.7777	0.5277	1.8680
150	0.6855	0.4355	1.4026
200	0.6523	0.4023	1.1666
250	0.6055	0.3555	0.9903
300	0.5928	0.3428	0.9149
350	0.5681	0.3181	0.8192
400	0.5352	0.2852	0.7224
450	0.5389	0.2889	0.6962
500	0.5128	0.2628	0.6301
600	0.4982	0.2482	0.5897
700	0.4753	0.2253	0.5262
800	0.4629	0.2129	0.4649
1000	0.4382	0.1882	0.4012

Table 10. Simulation Data for Alpha (set4)

Sample size	MLE	Bias	MSE
50	26.2432	1.2432	81.1398
70	25.3049	0.3049	49.2402
100	24.9138	-0.0861	35.3313
150	24.6671	-0.3328	24.0662
200	24.4205	-0.5794	18.6310
250	24.3793	-0.6206	15.9575
300	24.3237	-0.6762	14.5665
350	24.2952	-0.7048	13.2150
400	24.2989	-0.7011	11.5578
450	24.2795	-0.7204	11.1183
500	24.2762	-0.7237	10.5934
600	24.3141	-0.6858	8.8860
700	24.3978	-0.6021	7.8518
800	24.4117	-0.5882	6.8631
1000	24.4597	-0.5402	5.7236

Table 11. Simulation Data for Beta (set4)

Sample size	MLE	Bias	MSE
50	1.9069	-0.0931	0.0933
70	1.9013	-0.0986	0.0835
100	1.9032	-0.0967	0.0742
150	1.9072	-0.0927	0.0628
200	1.9034	-0.0965	0.0589
250	1.9110	-0.0889	0.0520
300	1.9101	-0.0898	0.0502
350	1.9146	-0.0853	0.0461
400	1.9215	-0.0784	0.0411
450	1.9209	-0.0790	0.0404
500	1.9243	-0.0756	0.0385
600	1.9289	-0.0710	0.0337
700	1.9359	-0.0640	0.0295
800	1.9385	-0.0614	0.0264
1000	1.9450	-0.0549	0.0227

Table 12. Simulation Data for Lambda (set4)

Sample size	MLE	Bias	MSE
50	0.8887	0.7387	2.6060
70	0.8021	0.6521	1.9793
100	0.7430	0.5930	1.6161
150	0.6736	0.5236	1.3222
200	0.6604	0.5104	1.2260
250	0.6082	0.4582	1.0579
300	0.6009	0.4509	0.9983
350	0.5717	0.4217	0.8971
400	0.5322	0.3822	0.7907
450	0.5351	0.3851	0.7728
500	0.5123	0.3623	0.7177
600	0.4846	0.3346	0.6464
700	0.4509	0.3009	0.5574
800	0.4341	0.2841	0.4891
1000	0.3998	0.2498	0.4154

5. Application to real dataset

In our investigation of the PISG distribution, we have analyzed two authentic datasets. To gauge the efficacy of our proposed model, we have conducted a comparative analysis against several established models with their PDF outlined below:

a. **GZ (Gompertz Distribution)** (Murthy et al., 2003) [19]:

$$f_{GZ}(t) = \theta\, e^{\alpha t}\, exp\left\{\left(1 - e^{\alpha t}\right)\frac{\theta}{\alpha}\right\} \quad ; t \geq 0, \theta > 0, -\infty < \alpha < \infty.$$

b. SGZ (Shifted Gompertz) distribution (Bemmaor, 1992) [20]:

$$f_{SGZ}(t;\alpha,\beta)=\beta\exp(-\beta x-\alpha e^{-\beta t})\left\{1+\alpha(1-e^{-\beta t})\right\};t\geq 0,(\alpha\beta)>0.$$

c. GEE (Generalized exponential extension) distribution (Lemonte, 2013) [21]:

$$f_{GEE}(t;\alpha,\beta,\lambda)=\alpha\lambda\beta\,(1+\lambda t)^{\alpha-1}\,exp\left\{1-(1+\lambda t)^{\alpha}\right\}\left[1-exp\left\{1-(1+\lambda t)^{\alpha}\right\}\right]^{\beta-1};\ t\geq 0.$$

d. WE (Weibull extension) model (Tang et al., 2003) [22]**:**

$$f_{WE}(t;\alpha,\beta,\lambda)=\lambda\beta\left(\frac{t}{\alpha}\right)^{\beta-1}\exp\left(\frac{t}{\alpha}\right)^{\beta}\exp\left\{-\lambda\alpha\left(\exp\left(\frac{t}{\alpha}\right)^{\beta}-1\right)\right\}\ ;\ t>0,\ \alpha>0,\beta>0\text{ and }\lambda>0.$$

e. GR (Generalized Rayleigh (GR) distribution (Kundu & Raqab, 2005) [23]:

$$f_{GR}(t;\ \alpha,\ \lambda)=2\,\alpha\,\lambda^2\,t\,e^{-(\lambda t)^2}\left\{1-e^{-(\lambda t)^2}\right\}^{\alpha-1}\quad;(\alpha,\lambda)>0,t>0.$$

For model selection, we have employed various criteria such as the Bayesian Information Criterion (BIC), Hannan-Quinn Information Criterion (HQIC), Akaike Information Criterion (AIC), Negative Log-Likelihood (-LL), and Corrected AIC (CAIC) statistics. These metrics are calculated using the following expressions:

$$AIC=-2\ell(\hat{\rho})+2h,$$
$$BIC=-2\ell(\hat{\rho})+h\log(n),$$
$$CAIC=\frac{2h(h+1)}{n-h-1}+AIC,$$
$$HQIC=-2\ell(\hat{\rho})+2h\log\left[\log(n)\right].$$

Here, let's define the estimated parameter space as $\hat{\rho}$, where 'n' represents the size of the sample, and 'h' denotes the parameter number of the model being investigated. To evaluate the goodness-of-fit for the proposed model, we have employed three statistical tests: the Cramer-Von Mises test (A^2), the Kolmogorov-Smirnov test (KS), and the Anderson-Darling test (W). The results of these tests are calculated as follows:

$$KS=\max_{1\leq m\leq n}\left(d_m-\frac{m-1}{n},\frac{m}{n}-d_m\right),$$
$$W=-n-\frac{1}{n}\sum_{m=1}^{n}(2m-1)\left[\ln d_m+\ln\left(1-d_{n+1-m}\right)\right],$$
$$A^2=\frac{1}{12n}+\sum_{m=1}^{n}\left[\frac{(2m-1)}{2n}-d_m\right]^2,$$

where x_m are the ordered observations, and $d_m=F\left(x_{(m)}\right)$.

5.1 Engineering data (data set 1)

The dataset was initially examined by (Bader & Priest, 1982) [24]. It encompasses the strength, measured in GPA, of single carbon fibers with a gauge length of 10 mm and a size of 69. The recorded values are as follows:

"1.312, 1.314, 1.479, 1.552, 1.700, 1.803, 1.861, 1.865, 1.944, 1.958, 1.966, 1.997, 2.006, 2.021, 2.027, 2.055, 2.063, 2.098, 2.14, 2.179, 2.224, 2.240, 2.253, 2.270, 2.272, 2.274, 2.301, 2.301, 2.359, 2.382, 2.382, 2.426, 2.434, 2.435, 2.478, 2.490, 2.511, 2.514, 2.535, 2.554, 2.566, 2.57, 2.586, 2.629, 2.633, 2.642, 2.648, 2.684, 2.697, 2.726, 2.770, 2.773, 2.800, 2.809, 2.818, 2.821, 2.848, 2.88, 2.954, 3.012, 3.067, 3.084, 3.090, 3.096, 3.128, 3.233, 3.433, 3.585, 3.585".

Estimation of the Model Parameters

The parameters of the proposed model were estimated using the R programming software (R Core Team, 2023) [25]. Table 13 displays the MLEs, LSEs, and CVEs for the PISG distribution, as defined by (Sapkota and Kumar, 2023) [26]. Figure 6 presents the log-likelihood profile for the model's parameters, confirming the existence and uniqueness of the MLEs. Additionally, we evaluated the model's fit using the KS, W, and A^2 statistics, alongside their respective p-values for the MLE, LSE, and CVE approaches. The findings are summarized in Table 14. Notably, for dataset 1, the results from all three estimation methods are strikingly similar.

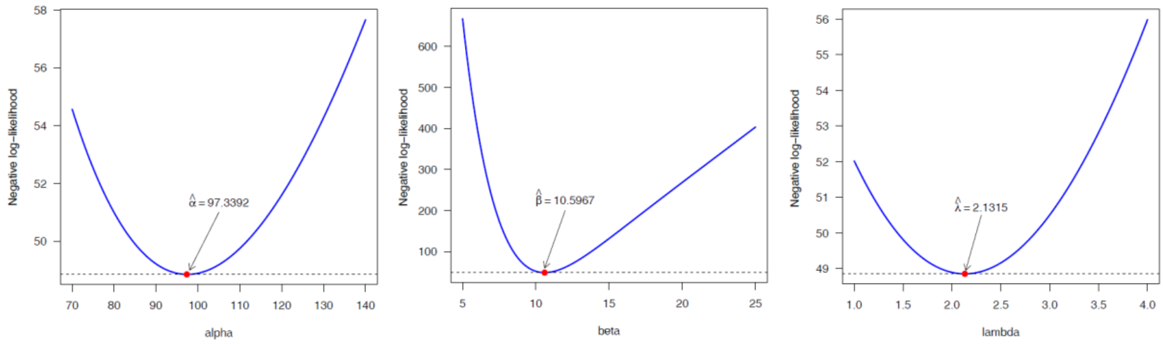

Figure 6. Graphs of Profile for α, β and λ (dataset 1).

Table 13. Estimated parameters, and fit statistics (dataset 1).

Method	$\hat{\alpha}$	$\hat{\beta}$	$\hat{\lambda}$	**-LL**	**AIC**	**BIC**
MLE	97.3392	10.5967	2.1315	48.8532	103.7064	110.4087
LSE	105.9969	11.0528	1.7312	48.8725	103.7449	110.4472
CVE	129.2641	11.6696	1.5235	48.8525	103.7051	110.4074

Table 14. Comparison of estimation methods (dataset 1).

Method	***KS(p-value)***	***A^2(p-value)***	***W(p-value)***
MLE	0.0378(0.9999)	0.1332(0.9995)	0.0147(0.9997)
LSE	0.0381(0.9999)	0.1378(0.9993)	0.0149(0.9997)
CVE	0.0386(0.9999)	0.1398(0.9992)	0.0139(0.9998)

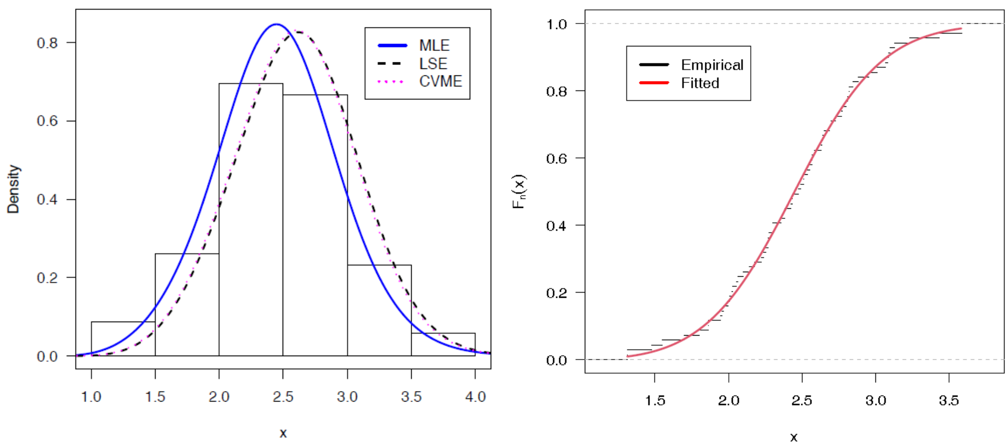

Figure 7. Fitted estimation methods (left) and KS plot of PISG (right) (dataset 1).

Assessment of Model Validity

In order to assess the validity of the PSIG model, we utilized the KS statistic, which measures the disparity between a fitted distribution and empirical distribution functions. Our analysis yielded a KS statistic of 0.0883 with a corresponding p-value of 0.7102 for the PISG model, indicating a favorable fit. This conclusion is further supported by the P-P and Q-Q plots (Figure 8) as well as the KS plot (Figure 9, right panel).

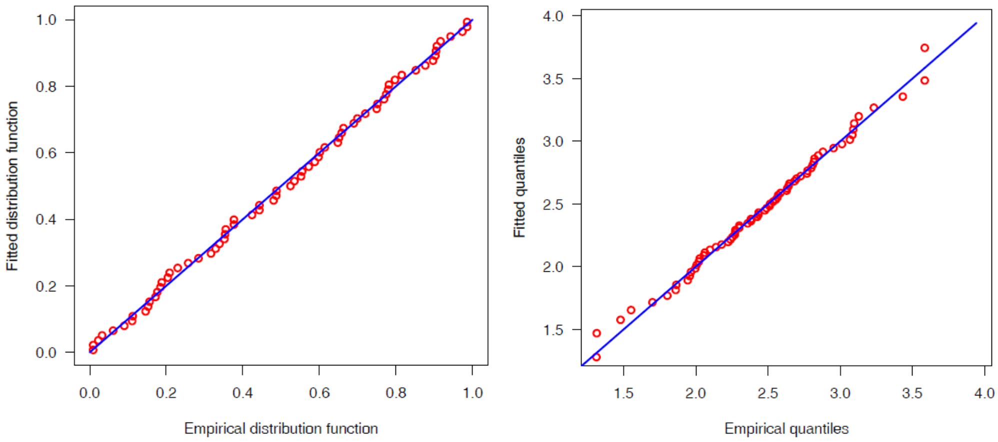

Figure 8. The P-P (left) and Q-Q plots (right) of the PISG distribution (dataset 1).

Model Adequacy and Goodness-of-Fit Evaluation

In our pursuit of identifying the most suitable model, we have conducted a comparative analysis involving five established models from the existing literature. Specifically, we have computed and presented the values of several statistical measures, namely the AIC, LL, BIC, HQIC, and CAIC, as outlined in Table 15.

Our analysis reveals that the proposed model consistently yields the lowest values across these statistical metrics. This suggests that our model outperforms the alternatives, namely WE, GEE, GR, GZ, and SGZ. To further substantiate our findings, we have visualized the goodness-of-fit comparison between the PISG distribution and the competing distributions, as depicted in Figure 9. In assessing goodness-of-fit, we have calculated the KS, W, and A^2 statistics, as summarized in Table 16. Upon careful examination of the results, it becomes evident that the PISG distribution exhibits the lowest test statistic values and higher p-values among the compared distributions. This compelling evidence leads us to the conclusion that the PISG distribution not only performs superiorly but also demonstrates greater consistency compared to the alternative distributions used for comparison.

Table 15. Different criteria for model selection.

Model	AIC	-LL	BIC	CAIC	HQIC
PISG	119.0565	56.5282	125.4859	119.4633	121.5852
WE	120.1261	57.0630	126.5555	120.5328	122.6548
GEE	118.4105	57.2052	122.6967	118.6105	120.0963
GR	119.9929	57.9964	124.2792	120.1929	121.6787
GZ	129.9731	61.9865	136.4025	130.3798	132.5018
SGZ	142.6598	69.3299	146.9461	142.8533	144.3456

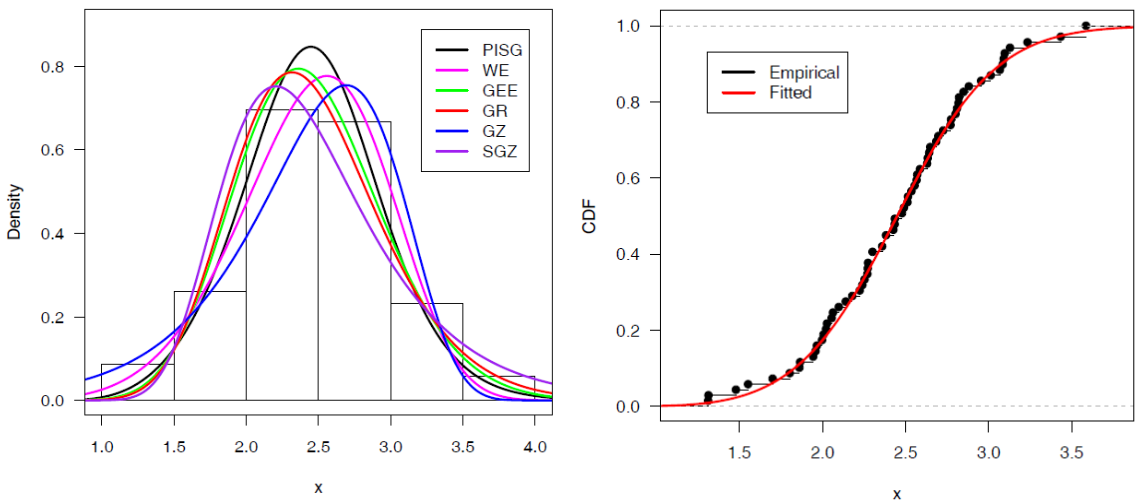

Figure 9: The fitted PDF and the Histogram (left panel) and Empirical with estimated CDF (right panel) of PISG distribution.

Table 16. Some statistics of the fitted models

Model	*KS(p-value)*	*W(p-value)*	*A^2(p-value)*
PISG	0.0883(0 .7102)	0.0704(0.7509)	0.3632(0.8839)
WE	0.0907(0.6784)	0.0714(0.7451)	0.4002(0.8480)
GEE	0.0635(0.9613)	0.0543(0.8516)	0.4044(0.8438)
GR	0.0919(0.6613)	0.0764(0.7144)	0.4613(0.7859)
GZ	0.0879(0.7148)	0.12498(0.4771)	0.9381(0.3911)
SGZ	0.1443(0.1452)	0.3504(0.0978)	2.3516(0.0595)

5.2 Medical data (data set 2)

This dataset, initially reported by (Clark and Gross, 1975) [27], has been utilized by (Chaudhary et al, 2023) [28]. It provides information on the relief times experienced by 20 patients after receiving an analgesic. The dataset consists of the following data points:

"1.1, 1.4, 1.3, 1.7, 1.9, 1.8, 1.6, 2.2, 1.7, 2.7, 4.1, 1.8, 1.5, 1.2, 1.4, 3.0, 1.7, 2.3, 1.6, 2.0"

Model Parameter Estimation

Table 17 presents the LSEs and CVMEs for the proposed model, along with their respective standard errors (SE). Additionally, Table 18 reports the MLEs for the PISG distribution. Figure 10 illustrates the performance comparison of the three estimation methods. It is noteworthy that these methods exhibit similar performance for the second dataset as well.

Table 17. LSEs and CVMs of PISG distribution (data set 2).

LSEs	SE	CVMs	SE
9.3416	19.0838	10.5459	22.9418
1.8907	12.8384	2.0738	10.4126
23.3734	510.6789	23.2756	374.6652

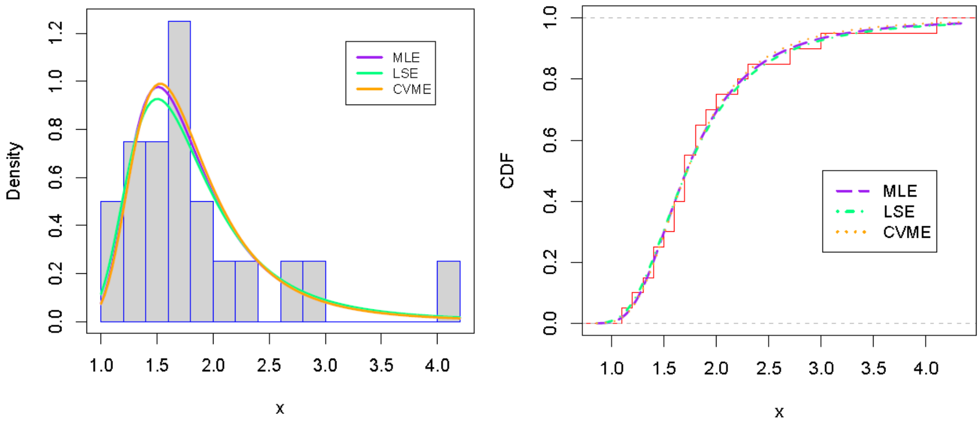

Figure 10. Fitted PDF and CDF for the estimation methods (data set 2).

Table 18. Estimated parameters with standard errors (data set 2).

Models		**MLEs (SE)**	
PSIG$(\hat{\alpha},\hat{\beta},\hat{\lambda})$	9.8117 (2.6233)	1.807 (1.4246)	32.7185 (87.1560)
GZ$(\hat{\alpha},\hat{\theta})$	0.8944 (0.2011)	0.1453 (0.0643)	--
SGZ$(\hat{\alpha},\hat{\beta})$	38.9615 (26.2869)	2.2782 (0.4227)	--
GEE$(\hat{\alpha},\hat{\beta},\hat{\lambda})$	0.4793 (0.1354)	1253.826 (3240.794)	49.1790 (91.1313)
WE$(\hat{\alpha},\hat{\beta},\hat{\lambda})$	89.203 (476.191)	2.7843 (0.4223)	368.0661 (3407.1670)

GR$(\hat{\alpha},\hat{\lambda})$	3.2460 (1.3208)	0.6911 (0.0857)	--

Assessment of Model Validity

In our analysis, we determined that the KS statistic (KS = 0.0951) and the corresponding p-value (p = 0.9936) for the PISG model demonstrate a strong level of fit. This conclusion is further supported by the visual representation of the Q-Q plot (on the left) and the KS plot (on the right) presented in Figure 11, both of which affirm the robustness of our results.

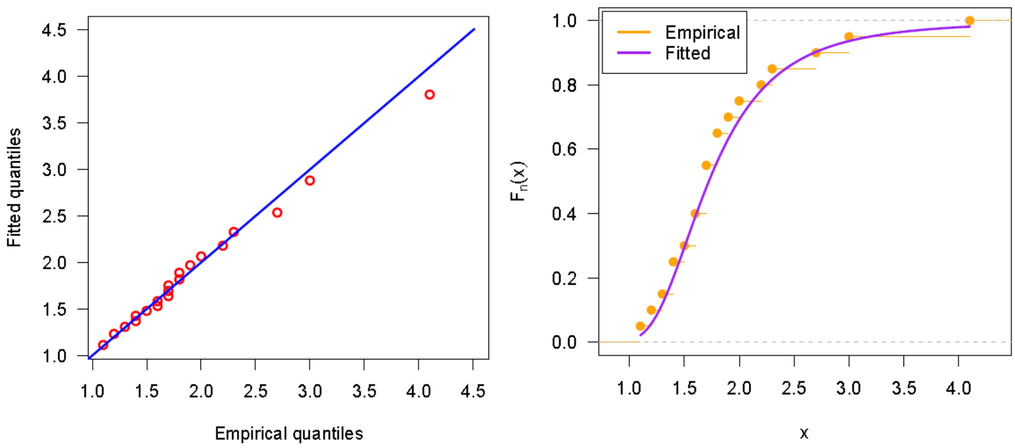

Figure 11. The Q-Q and KS plots of PISG distribution (data set 2).

Model Selection

In our selection process, we performed various goodness-of-fit tests, including the KS, A^2 and W test. Additionally, we utilized model selection criteria such as the AIC and LL. Our findings, as presented in Table 19, reveal that the PISG distribution exhibits the lowest test statistic value and the highest p-value. Based on these results, we can confidently assert that the PISG distribution outperforms and demonstrates greater consistency than the other distributions considered for comparison. To further reinforce this conclusion, we have included a graphical representation of the goodness-of-fit comparisons between the PISG distribution and its competitors in Figure 12, which substantiates the superiority of the PISG model among the candidate models.

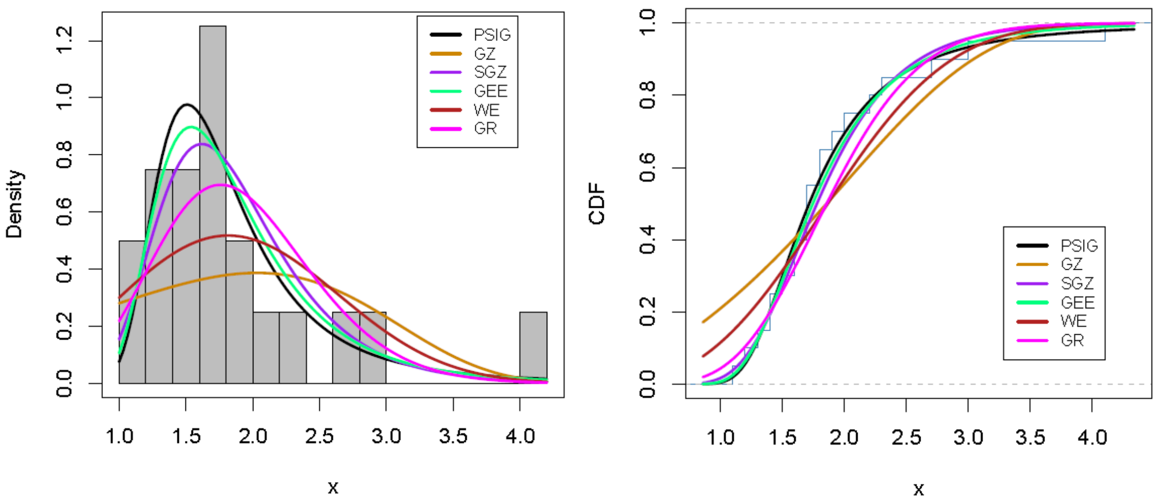

Figure 12. The fitted PDF with the Histogram (left panel) and Empirical with estimated CDF (right panel) of PISG distribution (data set 2).

Table 19. Model selection statistics for the data set 2.

Models	-2logL	AIC	KS (p-value)	W (p-value)	A^2 (p-value)
PSIG	30.9293	36.9293	0.0951 (0.9936)	0.0240 (0.9929)	0.1429 (0.9991)
GZ	49.1802	53.1802	0.2382 (0.2064)	0.3147 (0.1225)	1.8059 (0.1183)
SGZ	32.6624	36.6624	0.1341 (0.8645)	0.0476 (0.8960)	0.3183 (0.9230)

GEE	31.1066	37.1066	0.1085 (0.9726)	0.0302 (0.9783)	0.1855 (0.9940)
WE	41.1733	47.1733	0.1847 (0.5023)	0.1834 (0.3036)	1.0836 (0.3154)
GR	36.8045	40.8045	0.1901 (0.4651)	0.1273 (0.4702)	0.7347 (0.5287)

6. Analysis of PSIG model under the Bayesian approach

In order to conduct a Bayesian analysis, it is essential to define the prior distribution, likelihood function, and posterior distribution. For our examination of the PSIG model, we have established these functions in the following manner:

Prior Distribution: For this study, we have adopted a Gamma prior distribution (weakly-informative) for the model parameters denoted as $\theta = (\alpha, \beta, \lambda)$ as $\alpha \sim G(c_1, d_1)$, $\beta \sim G(c_2, d_2)$ and $\lambda \sim G(c_3, d_3)$ where $(c_1 = 0.5,\ d_1 = 0.5)$, $(c_2 = 0.1,\ d_2 = 0.1)$ and $(c_3 = 0.1,\ d_3 = 0.1)$ respectively. The choice of this Gamma prior aligns with common practice for introducing weak prior information on variance, as study by (Gelman et al., 2013) [29].

Likelihood: The likelihood function plays a crucial role in our study by quantifying the probability of observing a specific dataset, given the model parameters. When we have a dataset $\underline{x} = (x_1, \ldots, x_n)$, the likelihood function can be mathematically represented as follows:

$$L(\alpha,\beta,\lambda/\underline{x}) = \left(\frac{\beta\lambda}{1-e^{-\lambda}}\right)^n \prod_{i=1}^{n}\left[x_i^{-2}\left\{1+\alpha\left(1-e^{-\beta/x_i}\right)\right\}\exp\left(-\frac{\beta}{x_i}-\alpha e^{-\beta/x_i}\right)\right]$$
$$\exp\left\{-\lambda\left(1-e^{-\beta/x_i}\right)\exp(-\alpha e^{-\beta/x_i})\right\}.$$

Posterior distribution:

The posterior distribution $p(\theta/data)$ of PISG distribution is defined as

$$p(\alpha,\beta,\lambda/\underline{x}) \propto \alpha^{a_1-1}\beta^{n+a_2-1}\lambda^{n+a_3-1}\exp(-b_1\alpha - b_2\beta - b_3\lambda)\prod_{i=1}^{n}\left[x_i^{-2}\left\{1+\alpha\left(1-e^{-\beta/x_i}\right)\right\}\exp\left(-\frac{\beta}{x_i}-\alpha e^{-\beta/x_i}\right)\right]\times$$
$$\exp\left\{-\lambda\left(1-e^{-\beta/x_i}\right)\exp(-\alpha e^{-\beta/x_i})\right\}.$$

In this study, we apply Markov Chain Monte Carlo (MCMC) techniques using Stan, a probabilistic programming framework developed by the (Stan Development Team, 2022) [30]. We specifically use the Hamiltonian Monte Carlo (HMC) method, along with its adaptive variant, the no-U-turn sampler (NUTS). For further details on these algorithms, see (Hoffman and Gelman, 2014) [31] and (Carpenter, 2016) [32].

To perform the analysis, we use dataset 1, as described in Section 5. The Stan models are executed within the R environment using the RStan package (Stan Development Team, 2022) [33], which incorporates both the HMC method and the NUTS engine. Four chains are run, each with 2000 iterations. By default, Stan produces 1000 warm-up iterations followed by 1000 sampling iterations for each chain, which are then used for inference.

Efficiency and convergence diagnostics for NUTS/ HMC.

Table 20. Informational statistics of NUTS/HMC

	accept_stat	stepsize	treedepth	n_leapfrog	divergent	energy
All chains	0.94	0.13	3.47	18.19	0.00	64.81
chain1	0.92	0.15	3.33	6.13	0.00	64.81
chain2	0.95	0.12	3.54	19.08	0.00	64.94
chain3	0.95	0.12	3.51	18.96	0.00	64.81
chain4	0.95	0.13	3.49	18.60	0.00	64.68

All the information related to sampling are reported in Table 20 and Table 21. From the both tables we found that sampling is efficient and there are no divergent transitions for detail (see Betancourt, 2017) [34].

Table 21. MCMC sampling information.

Parameter	Rhat	se_mean/sd	n_eff/N	n_eff	Tail_ESS	Bulk_ESS
alpha	1.00	0.03	0.26	1029	1483	1008
beta	1.00	0.03	0.23	914	959	915
lambda	1.00	0.03	0.22	897	1291	1105
log-posterior	1.00	0.03	0.31	1230	1724	1393

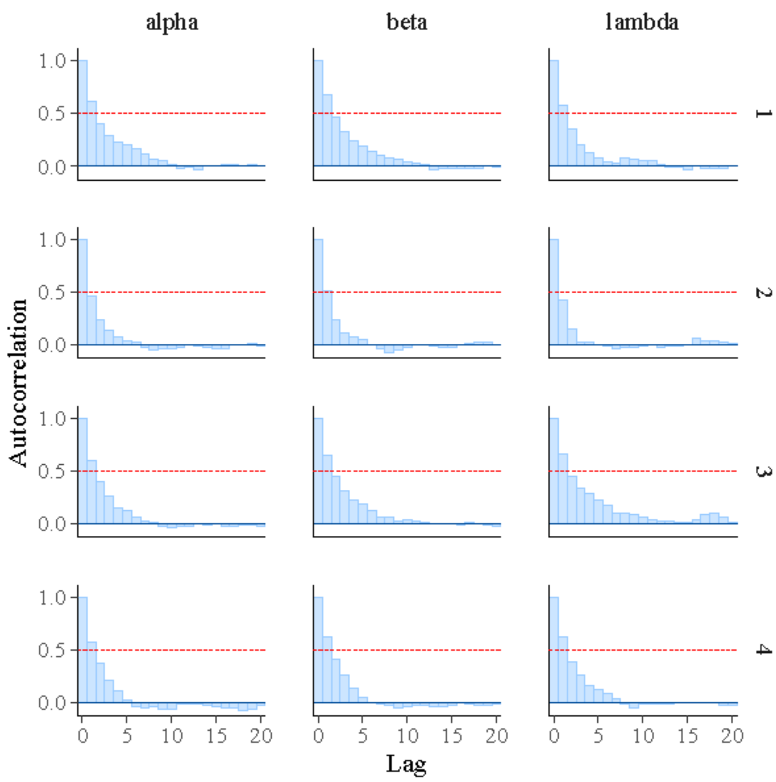

Figure 13. Autocorrelation plots (ACP) of the parameters α, β *and* λ for all 4-chains.

Figure 13 displays the ACP for α, β *and* λ all chains, indicating the independence of the samples. To further assess the convergence of these chains, we have generated trace plots. Trace plots offer a visual means to evaluate sampling performance and mixing crosswise chains. Figure 14 illustrates the trace plots, demonstrating that the chains exhibit good mixing and convergence across all chains. For more details, please refer to (Vehtari et al., 2019) [35].

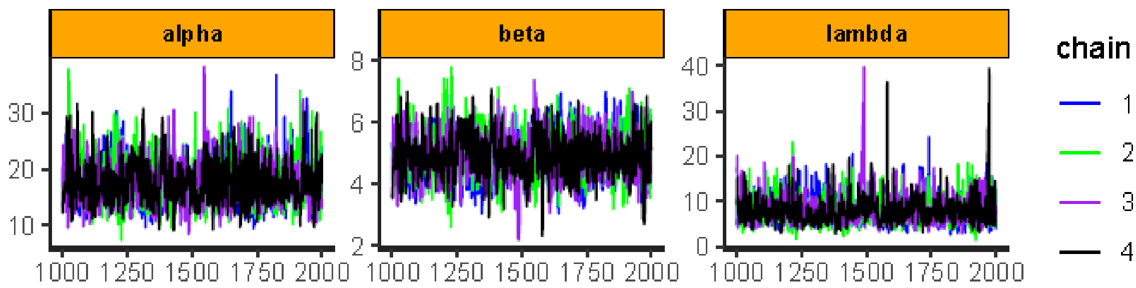

Figure 14. Trace plots of the parameters α, β *and* λ .

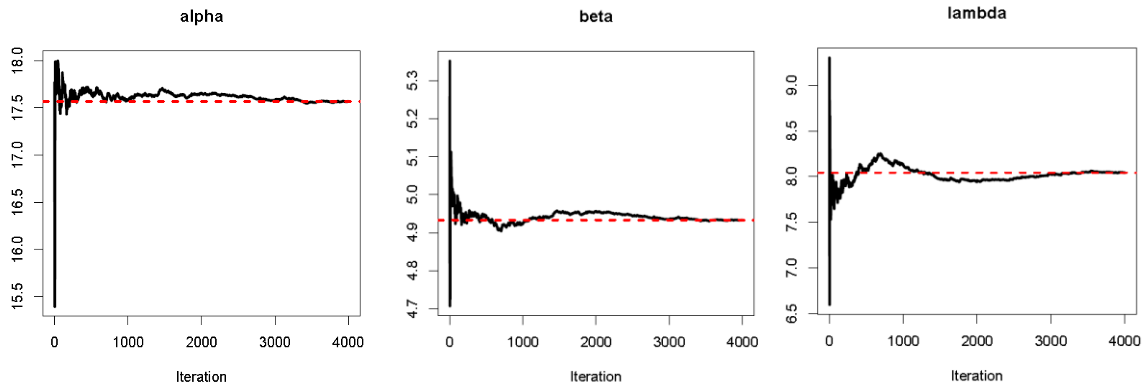

Figure 15. Ergodic average plot for the parameter of the PSIG.

The Ergodic average is determined by calculating the mean of sample values from all iterations across multiple chains. As depicted in Figure 15, all chains exhibit a smooth convergence towards the mean value (highlighted by the red dotted line). In Figure 16, a bivariate plot showcases the MCMC draws, and no signs of divergent transitions are apparent. In the plot, any draws shown in red color would indicate the presence of divergent transitions.

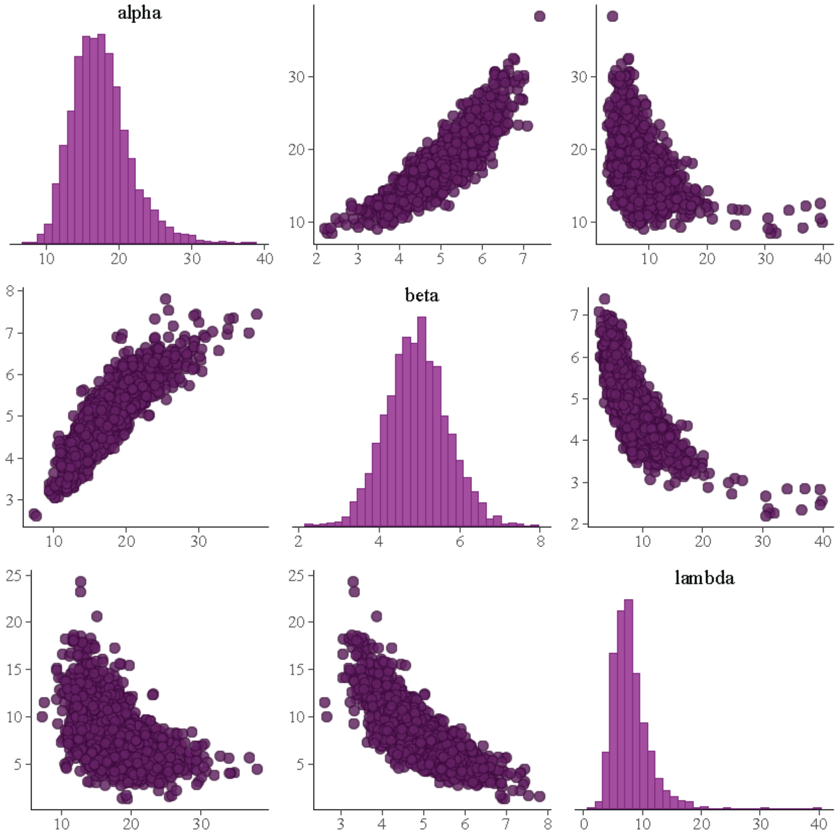

Figure 16. Pairs plot of α, β *and* λ .

Posterior Analysis:

We utilized the **`stan()`** function within the R-Software to compute the posterior density for our fitted PISG model. In Table 22, we have provided a comprehensive summary of the posterior results, encompassing key statistics such as the posterior mean estimates, the standard error derived from Monte Carlo simulations (se_mean), the posterior standard deviation (sd) across all merged chains. Additionally, we have included quantiles for both the median (50%) and the 95% credible interval (CI) (2.5%, 97.5%) for a more thorough understanding of the distribution.

It is noteworthy that none of the model parameters exhibit an effective sample size (n_eff) for obtaining the posterior mean that falls below 10% of the total sample size. This observation indicates the efficiency of our sampling procedure. Furthermore, the Rhat statistic, an estimate of the potential scale reduction factor, has values consistently below 1.1 for all chains. This signifies the convergence of all chains in our analysis, underlining the reliability of our results.

Table 22. Descriptive statistics of posterior samples for the PISG model.

Parameters	mean	se_mean	sd	2.5%	50%	97.5%	n_eff	Rhat
alpha	17.57	0.12	3.91	11.31	17.21	26.62	1027	1.0
beta	4.93	0.02	0.75	3.48	4.92	6.46	913	1.0
lambda	8.04	0.11	3.22	3.77	7.51	15.58	895	1.0
Log-posterior	-63.37	0.04	1.24	-66.46	-63.07	-61.96	1228	1.0

We have generated kernel density estimates for α, β *and* λ using all four chains in Figure 17. This figure illustrates the kernel density estimates along with a 95% CI (indicated by the red line). Notably, the parameter β appears to exhibit a near-symmetric distribution, while both α and λ exhibit positively skewed distributions.

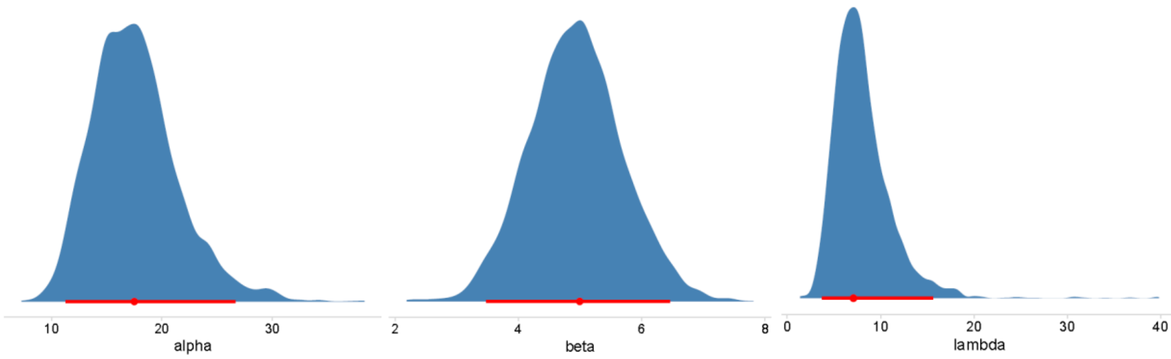

Figure 17. Density plots with 95% credible interval (red line with mode).

Additionally, we have generated a caterpillar plot - a widely utilized visualization tool in Bayesian analysis for summarizing posterior sample quantiles. In Figure 18, it was observed that the caterpillar plot, featuring a 90% CI represented by the blue line and a 99% CI indicated by the green line, with the default point estimate being the median.

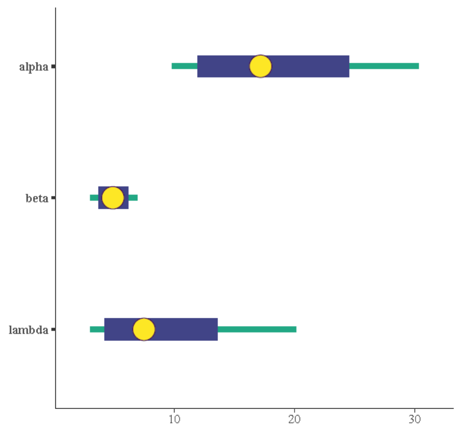

Figure 18. Caterpillar plot featuring a 90% CI represented by the blue line, a 99% CI indicated by the green line, with median point.

7. Concluding remarks

In this research endeavor, we introduce a novel distribution derived from the truncated Poisson family, which we have coined as the "Poisson Inverted Shifted Gompertz" (PISG) distribution. Our exploration includes the derivation of explicit expressions for various essential statistical properties, such as the reliability function, hazard rate function, moments, average residual life function, quantile function, entropies, order statistics, skewness, and kurtosis. To estimate the parameters of the proposed PISG model, we employ three different estimation methods: the LSE, MLE, and CVME. Our findings indicate that all three estimation techniques yield satisfactory results for our research objectives. To gain further insight into the behavior of MLE, we conduct a comprehensive simulation study. To showcase the practical utility of the PISG distribution, we apply it to two real-world datasets originating from engineering and medical domains. Our analysis demonstrates that the PISG model exhibits a better fit compared to five alternative models that were considered for comparison.

Additionally, we employ Stan software, featuring MCMC techniques based on the NUTS, an adaptive variant of HMC. This advanced sampler allows for a robust and efficient Bayesian analysis of the PISG distribution. We provide both numerical and graphical analyses of the PISG model using posterior samples, confirming the convergence and mixing of all chains. The techniques we have developed are not only applied to observed datasets but also serve as a foundation for a comprehensive Bayesian analysis of the PISG model. This demonstrates the versatility and applicability of our research methods for a wide range of statistical inquiries.

Authors' Contributions:
Authors have worked equally to write and review the manuscript.

Data Availability Statement:
The data that supports the findings of this study are available within the article.

Conflicts of Interest:
The authors declare no conflict of interest.

Reference

1. Kus, C. (2007). A new lifetime distribution. *Computational Statistics and Data Analysis* 51, 4497-4509.
2. Bereta, E. M., Louzanda, F., & Franco, M. A. (2011). The poisson-weibull distribution. *Adv. Applic. Statist*, *22*(2), 107-118.
3. Barreto-Souza, W. and Cribari-Neto, F. (2009). A generalization of the exponential-Poisson distribution. *Statistics and Probability Letters,* 79, 2493-2500.
4. Cancho, V. G., Louzada-Neto, F. and Barriga, G. D. C. (2011). The Poisson-exponential lifetime distribution. *Computational Statistics and Data Analysis,* 55, 677-686.
5. Alkarni, S. and Oraby, A. (2012). A compound class of Poisson and lifetime distributions, *J. Stat. Appl. Pro*., 1(1), 45-51.
6. Louzada-Neto, F., Cancho, V.G. & Barriga, G.D.C. (2011). The Poisson–exponential distribution: a Bayesian approach, *Journal of Applied Statistics*, *38*(6), 1239-1248.
7. Morais, A. L., & Barreto-Souza, W. (2011). A compound class of Weibull and power series distributions. *Computational Statistics & Data Analysis*, *55*(3), 1410-1425.
8. Lu, W. & Shi, D. (2012). A new compounding life distribution: the Weibull–Poisson distribution, *Journal of Applied Statistics*, 39:1, 21-38.
9. Mahmoudi, E., & Sepahdar, A. (2013). Exponentiated Weibull–Poisson distribution: Model, properties and applications. *Mathematics and computers in simulation*, *92*, 76-97.
10. Kaviayarasu, V. & Fawaz, P. (2017). A Reliability Sampling Plan to ensure Percentiles through Weibull Poisson Distribution, *International Journal of Pure and Applied Mathematics*, 117(13), 155-163.
11. Kyurkchiev, V. E. S. S. E. L. I. N., Kiskinov, H. R. I. S. T. O., Rahneva, O. L. G. A., & Spasov, G. E. O. R. G. I. (2018). A Note on the Exponentiated Exponential-Poisson Software Reliability Model. *Neural, Parallel, and Scientific Computations*, *26*(3), 257-267.
12. Chaudhary, A. K. & Kumar, V. (2020). Poisson Inverse NHE Distribution with Theory and Applications. *International Journal of Science and Research (IJSR),* 9(12), 1603-1610.
13. Joshi, R. K. & Kumar, V. (2020). Poisson Exponential Power distribution: Properties and Application. *International Journal of Mathematics & Computer Research* 8(11), 2152-2158
14. Chaudhary, A. K., Sapkota, L. P., & Kumar, V. (2021). Poisson Gompertz Distribution with Properties and Applications. *International Journal of Applied Engineering Research*, *16*(1), 75-84.
15. Wasinrat, S., & Choopradit, B. (2023). The Poisson Inverse Pareto Distribution and Its Application. *Thailand Statistician*, *21*(1), 110-124.
16. Sapkota, L. P. (2022). A Bayesian Analysis and Estimation of Weibull Inverse Rayleigh Distribution Using HMC Method. *Nepal Journal of Mathematical Sciences*, *3*(2), 39–58.
17. Chaudhary, A. K., Sapkota, L. P., & Kumar, V. (2020). Inverted Shifted Gompertz Distribution with Theory and Applications. *Pravaha*, *26*(1), 1-10.
18. Bemmaor, A. C. (1994). Modelling the diffusion of new durable goods: Word-of-mouth effect versus consumer heterogeneity. In: Laurent, G., Lilien, G. L., Pras, B., eds. *Research Traditions in Marketing*. Boston: Kluwer, pp. 201 – 229.
19. Murthy, D.N.P., Xie, M. and Jiang, R. (2003). *Weibull Models*, Wiley, New York.

20. Bemmaor, A. C. (1992). Modeling the diffusion of new durable goods: Word-of-mouth effect versus consumer heterogeneity. In *Research traditions in marketing* (pp. 201-229). Springer, Dordrecht.

21. Lemonte, A. J. (2013). A new exponential-type distribution with constant, decreasing, increasing, upside-down bathtub and bathtub-shaped failure rate function. *Computational Statistics & Data Analysis*, *62*, 149-170.

22. Tang, Y., Xie, M., & Goh, T. N. (2003). Statistical analysis of a Weibull extension model. *Communications in Statistics-Theory and Methods*, *32*(5), 913-928.

23. Kundu, D., and Raqab, M.Z. (2005). Generalized Rayleigh Distribution: Different Methods of Estimation, *Computational Statistics and Data Analysis*, 49, 187-200.

24. Bader, M. G., & Priest, A. M. (1982). Statistical aspects of fiber and bundle strength in hybrid composites. *Progress in science and engineering of composites*, 1129-1136.

25. R Core Team (2023). R: A language and environment for statistical computing. R Foundation for Statistical Computing, Vienna, Austria. URL https://www.R-project.org/.

26. Sapkota, L. P. & Kumar, V. (2023). Half Cauchy Generalized Rayleigh Distribution: Theory and Application. *South East Asian J. of Mathematics and Mathematical Sciences*, 19(1), 335-360.

27. Clark, V. A., & Gross, A. J. (1975). *Survival distributions: reliability applications in the biomedical sciences*. New York, John Wiley & Sons.

28. Chaudhary, A. K., Sapkota, L. P., & Kumar, V. (2023). Inverse Exponential Power distribution: Theory and Applications. International Journal of Mathematics, Statistics and Operations Research. 3(1), 175-185.

29. Gelman, A., Carlin, J.B., Stern, H.S., Dunson, D.B., Vehtari, A., & Rubin, D.B. (2013). Bayesian Data Analysis (3rd ed.). Chapman and Hall/CRC. https://doi.org/10.1201/b16018

30. Stan Development Team, (2023). Stan users guide, version 2.28; *https://mc-stan.org/docs/2_18/reference-manual/index.html.* Accessed 28 Oct 2022.

31. Hoffman, M. D., & Gelman, A. (2014). The No-U-Turn sampler: adaptively setting path lengths in Hamiltonian Monte Carlo. *J Mach Learn Res*, 15, 1593–1623.

32. Carpenter, B., Gelman, A., Hoffman, M., Lee, D., Goodrich, B., Betancourt, M., Brubaker, M.A., Guo, J., Li, P. & Riddell, A. (2016). Stan: A probabilistic programming language. *Journal of Statistical Software,* 20, 1-37.

33. Stan Development Team (2022). "RStan: the R interface to Stan." R package version 2.21.5, https://mc-stan.org/.

34. Betancourt, M., (2017). A Conceptual Introduction to Hamiltonian Monte Carlo. arXiv preprint arXiv:1701.02434.

35. Vehtari, A., Gelman, A., Simpson, D., Carpenter, B., & Bürkner, P. C. (2019). Rank-normalization, folding, and localization: An improved $\widehat {R} $ for assessing convergence of MCMC. *arXiv preprint arXiv:1903.08008*.